JOURNAL OF MATERIALS SCIENCE 26 (1991) 2769–2777

Correlation of microhardness and morphology of poly(ether–ether–ketone) films

Y. DESLANDES, E. ALVA ROSA*
Division of Chemistry, National Research Council of Canada, Ottawa, Ontario, Canada K1A 0R9

F. BRISSE, T. MENEGHINI
Département de Chimie, Université de Montréal, Montréal, Québec, Canada H3C 3J7

We have applied microindentation to a series poly(ether–ether–ketone) films crystallized at different temperatures from the melt and from the glass to measure their microhardness. The morphology of the samples was characterized by X-ray diffraction, density measurements and differential scanning calorimetry. The results show that a relationship between microhardness, density and degree of crystallinity can be established for samples crystallized at various temperatures from both the glass and the melt. The values of the microhardness of the crystalline component of the samples can be correlated with the lamellar thickness of the polymer crystals.

1. Introduction

Microindentation is a technique based on the Vickers indentor used to measure hardness and toughness of materials. The method employs a "pyramidally tipped" diamond indentor to penetrate the surface of a specimen upon the controlled application of a given load [1, 2]. After unloading, a residual surface impression is left on the specimen. From the dimensions of the impression, the microhardness of the materials can be calculated. Microindentation has been extensively used for characterizing metals and ceramics where it has been shown to be very sensitive to the chemical composition and microscopic structure of the materials. The application of the technique to polymeric systems is a relatively new approach, with great potential for the characterization of solid polymer.

During the last fifteen years, investigations of the microhardness properties of various polymers have evolved from rather straightforward technical aspects to more elaborate studies aimed at acquiring fundamental knowledge of the morphology–property relationship of polymeric systems [1, 2]. Although polyethylene has received most of the attention [3–17], microhardness measurements of other materials such as polypropylene [18, 19] poly(ethylene terephthalate) [19] polytetrafluoroethylene [19] and polycarbonate [20] as well as of copolymers [21] blends [22] and doped polymers [23] have been reported. These studies have clearly demonstrated that microhardness of semicrystalline polymers can be related to their microstructure. For example, microhardness of polyethylene has been shown to depend on the overall degree of crystallinity, the thickness of both the amorphous and crystalline regions of the lamellae as well as on the chain packing within the crystals [1]. Microindentation measurements have also led to the identification of different microstructural reorganization mechanisms occurring at various morphological levels [1–7]. From a more practical level, microindentation has also been successfully applied to characterize microstructural details of injection moulded thermoplastics [24].

Poly(ether–ether–ketone) (PEEK) is a semicrystalline polymer used in composites for high temperature structural applications. PEEK has a glass transition temperature of about 140 °C and melts at temperatures above 320 °C with an equilibrium melting temperature, $T_m^o > 389$ °C [25, 26]. PEEK is characterized by a complex crystallization behaviour. Double melting peaks similar to those observed for poly(ethylene terephthalate) are often recorded and changes in the Avrami exponent as crystallization proceeds have been reported [26, 27]. These crystallization features control the morphology and consequently the mechanical behaviour of PEEK.

We believe that microhardness could be advantageously applied to poly(ether–ether–ketone) to provide some important information on the structure–property relationship of this polymer. Since the method can be used on small sample size and is "quasi" non-destructive, it represents, in our opinion, an interesting research tool to help establishing the structure–property relationship of polymers samples which are made on a small scale in a research laboratory. In addition, once the fundamental data are acquired on PEEK, the method could find some very interesting technical applications in composites. High resolution mapping of the mechanical properties of a

* *Permanent address*: Department of Chemistry, Concordia University, Montreal, Quebec, Canada

0022–2461/91 $03.00 + .12

processed sample, the determination of skin–core effects, the measurement of crystallinity changes in "repaired areas" of large pieces as well as mechanical characterization of surface changes induced by oxidation or other deterioration processes represent interesting potential applications of the method.

To our knowledge, this is a first attempt at correlating the morphological characteristics and the microhardness of PEEK. Unfortunately, like all semicrystalline polymers, the relationship between the two is extremely complex. As discussed by Popli and Mandelkern [28], there are many parameters in addition to molecular factors that ultimately have an effect on the mechanical properties. A good understanding of the structure of the crystallites, their interrelations with one another as well as the structure of the chain segments connecting the lamellae is necessary to establish a model for the behaviour of these materials. It is thus important to consider variables which are controlled by the molecular weight, chain structure and crystallization conditions such as the degree of crystallinity, the crystallite structure, their thickness distribution, the structure and relative amount of the interfacial region of the non-crystalline region and the supermolecular structure [29].

In a recent article we reported the effect of the degree of crystallinity on microhardness for PEEK [30]. Our next objective was to examine in more detail the effect of some of the morphological features of the crystalline component on microhardness. We have tried to focus our attention on the lamellar thickness and the effect of the change in unit cell dimension with crystallization temperature observed for PEEK. In this study we have limited ourselves to the use of a commercial sample that was thermally treated under different conditions to induce different morphologies.

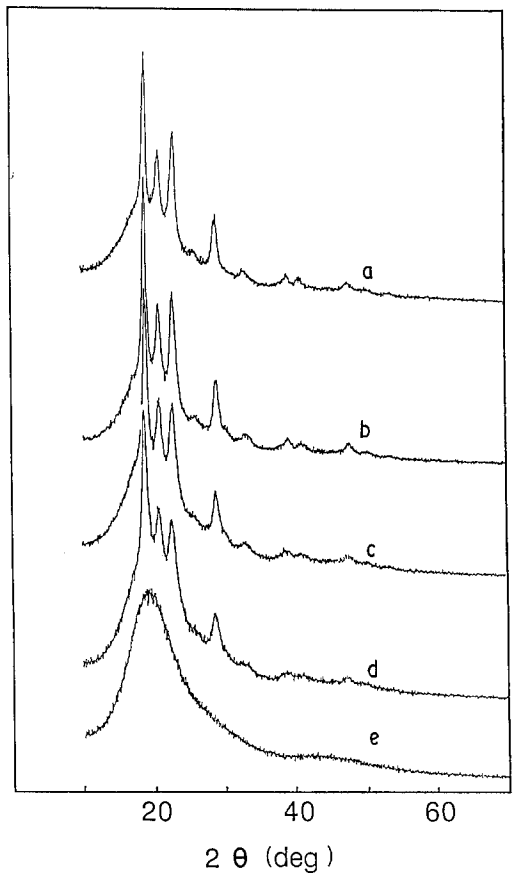

Figure 1 X-ray diffraction traces of some selected samples crystallized from the glass and the melt as well as the "as-received" amorphous film. For purposes of clarity, the curves have been translated along the intensity axis. (a $T_c = 323\,°C$ from the melt, b $T_c = 325\,°C$ from the glass, c $T_c = 276\,°C$ from the glass, d $T_c = 207\,°C$ from the glass, e amorphous PEEK film)

2. Experimental procedure

2.1. Samples

A PEEK film, STABAR K200, about 250 μm (10 mils) thick, supplied by ICI AMERICA, Wilmington, Delaware, USA, was selected for this study because of its uniform thickness and its smooth surface which is essential for accurate microhardness measurements [2]. The "as-received" film is transparent and X-ray diffraction indicates that it is amorphous (see Fig. 1). Small squares were cut $(2 \times 2\,cm)^2$, placed between two glass slides and crystallized in a glove box, under a nitrogen atmosphere, according to either of the following two procedures. For the procedure involving crystallization from the glassy state, the films were placed directly in a press heated to the desired specific temperature over the range 180 to 340 °C. No pressure was applied to the sample but the two heated platens were brought into contact with the glass slides to assure a good uniformity of temperature on both sides of the sample. The temperature was measured with a thermocouple placed beside the sample and is believed to be controlled to within $\pm 2\,°C$. After 1 h, the sample was removed from the press and allowed to cool to room temperature under a nitrogen atmosphere. The other procedure involved crystallization from the melt. The PEEK film was first melted at 400 °C on a hot plate, kept there for 1 min and then transferred to the press which had been heated to a preset temperature in the range of 270 to 340 °C. The sample was isothermally crystallized at this temperature for 1 h (except for the sample held isothermally at 329 °C which had not crystallized after 1 h and had to be kept at this temperature for 17 h to complete the crystallization). The sample was then removed and rapidly cooled to room temperature by placing it on a massive steel plate. A mould-release agent (Multi-release Mono Coat E-7A, Chem-Trend Inc. Howell, MI, USA) was sprayed onto the glass slide prior to heating the sample in order to inhibit adhesion between the polymer and the glass. The temperatures investigated in this study are summarized in Table I.

2.2. Microhardness Measurements

The microhardness measurements were carried out at room temperature using a Buehler Micromet II microhardness tester equipped with a diamond square pyramid having an angle at the tip of 68°. A load of 100 g was applied for 5 s. The length of the diagonals, d, of the diamond shaped indentation was measured immediately after the removal of the load using a micrometer eyepiece mounted on the microscope. The

TABLE I Characteristic features and microhardness of the samples

T_c (°C)	Density (g cm^{-3})	ϕ_c[a]	X_c[b]	h_{exp}[c] (J g^{-1})	X_h[d]	X_x[e]	l_c[f] (nm)	H[g] (MPa)
From the glass								
Untreated	1.2604	0	0	0	0	0	0	135
180	1.2855	0.262	0.277	38	0.292	0.205	1.7	208
207	1.2882	0.254	0.270	36.1	0.297	0.265	2.0	206
224	1.2917	0.289	0.307	43.5	0.334	0.304	2.1	216
253	1.2930	0.279	0.297	49.5	0.380	0.323	2.6	221
276	1.2946	0.283	0.302	48.8	0.375	0.332	3.1	232
301	1.2981	0.298	0.319	51.5	0.396	0.345	3.9	242
325	1.3005	0.305	0.326	48.7	0.374	0.426	5.2	243
340	1.3045	0.319	0.342	54.8	0.421	0.435	6.5	251
From the melt								
272	1.2996	0.305	0.326	43.6	0.336	0.415	2.9	241
286	1.3014	0.326	0.347	43.9	0.338	0.407	3.3	244
299	1.3022	0.325	0.347	44.2	0.340	0.434	3.7	247
310	1.3031	0.315	0.338	43.7	0.336	0.406	4.2	255
323	1.3036	0.319	0.342	44.9	0.345	0.389	5.0	256
329[h]	1.3054	0.305	0.330	42.9	0.330	0.384	5.5	290

[a] volume fraction crystallinity, [b] weight fraction crystallinity, [c] enthalpy of fusion, [d] crystallinity index from enthalpy of fusion, [e] crystallinity index from X-ray diffraction, [f] calculated lamellar thickness, [g] microhardness.
[h] annealed for 17 h

microhardness H was calculated using the following equation [2, 12]

$$H = (2 \sin 68°) \frac{P}{d^2} = 1.854 \frac{P}{d^2} \quad (1)$$

where P is the load applied and d the diagonal of the indentation.

2.3. Density Measurements

The density, ρ, of the samples was determined by the flotation method using water and calcium nitrate as proposed by Blundel and Osborn [25]. The measured density of the "as-received", amorphous, Stabar film was taken as the amorphous density ρ_a. This value is slightly lower than the density reported for amorphous PEEK, by Blundel and Osborn [25]. The crystalline density, ρ_c, for each sample, had to be calculated from the unit cell dimensions determined by the X-ray diffraction procedure described below (see Table II). This was necessary because of a change in unit cell with crystallization temperature [31, 32].

The apparent weight fraction crystallinity X_c was calculated using the equation

$$X_c = \frac{(\rho - \rho_a)}{(\rho_c - \rho_a)} \frac{\rho_c}{\rho} = \phi_c \frac{\rho_c}{\rho} \quad (2)$$

where $\phi_c = (\rho - \rho_a)/(\rho_c - \rho_a)$ is the volume fraction crystallinity.

2.4. Enthalpy of fusion

The experimental enthalpy of fusion, Δh_{exp}, was calculated from the area of the melting endotherm of the

TABLE II Unit cell parameters and density of fully crystalline component for PEEK samples heat treated at various temperatures. The unit cell is orthorhombic

T_c (°C)	a (nm)	b (nm)	c (nm)	Volume (nm^3)	Calculated density of fully crystalline sample
From the glass					
180	0.7963 (0.0016)	0.5932 (0.0012)	0.9954 (0.0016)	0.470 (0.005)	1.3559
207	0.7911 (0.0018)	0.5952 (0.0013)	0.9887 (0.0022)	0.465 (0.006)	1.3696
224	0.7901 (0.0012)	0.5929 (0.0009)	0.9945 (0.0015)	0.466 (0.004)	1.3684
253	0.7880 (0.0019)	0.5913 (0.0014)	0.9935 (0.0024)	0.462 (0.007)	1.3773
276	0.7848 (0.0010)	0.5915 (0.0007)	0.9943 (0.0010)	0.461 (0.003)	1.3811
301	0.7815 (0.0010)	0.5902 (0.0008)	0.9969 (0.0013)	0.459 (0.004)	1.3865
325	0.7757 (0.0010)	0.5909 (0.0008)	0.9995 (0.0014)	0.458 (0.004)	1.3917
340	0.7751 (0.0005)	0.5903 (0.0005)	0.9963 (0.0005)	0.455 (0.002)	1.3987
From the melt					
272	0.7799 (0.0004)	0.5911 (0.0003)	0.9958 (0.0005)	0.459 (0.001)	1.3887
286	0.7824 (0.0010)	0.5906 (0.0009)	0.9954 (0.0011)	0.460 (0.003)	1.3863
299	0.7808 (0.0010)	0.5918 (0.0007)	0.9936 (0.0012)	0.459 (0.003)	1.3887
310	0.7768 (0.0003)	0.5902 (0.0003)	0.9963 (0.0004)	0.457 (0.002)	1.3957
323	0.7742 (0.0010)	0.5909 (0.0007)	0.9986 (0.0013)	0.457 (0.004)	1.3957
329	0.7722 (0.0007)	0.5884 (0.0006)	0.9969 (0.0010)	0.453 (0.003)	1.4077

differential scanning calorimetry (DSC) trace. The traces were recorded with a DuPont model 910 differential scanning calorimeter coupled to a 2100 thermal analyser. Samples weighing approximately 6 mg placed in crimped aluminium sample pans were run in a nitrogen atmosphere employing a heating rate of $10\,^{\circ}C\,min^{-1}$. The nitrogen flow rate was $50\,ml\,min^{-1}$. The instrument was calibrated with indium and zinc. The value of Δh_{exp} was used in calculating the apparent crystallinity index X_h based on enthalpy of fusion according to Equation 3.

$$X_h = \frac{\Delta h_{exp}}{\Delta h_f} \quad (3)$$

In our study, a value of $130\,J\,g^{-1}$ was used for the enthalpy of fusion (Δh_f) of a completely crystalline sample as estimated by Blundel and Osborn [25].

2.5. X-ray diffraction

Wide angle X-ray scattering traces of the films were recorded with a powder X-ray diffractometer in reflection Bragg–Brentano flat plate geometry using Ni-filtered Cu$K\alpha$ radiation. The measured d spacings of nine reflections were used in refining the cell parameters for each sample assuming an orthorhombic unit cell (see Table II).

We applied the method proposed by Blundell and Osborn for the determination of the degree of crystallinity based on X-ray diffraction for PEEK [25]. The method consists in drawing an approximate amorphous curve under the diffraction trace and of calculating the ratio of the areas of the crystalline peaks to the total area between the 2Θ values of 10° and 36°. This ratio was taken as the weight fraction index for the X-ray crystallinity X_x.

The small angle X-ray scattering traces were obtained on a Rigaku–Denki small angle scattering goniometer using the nickel-filtered copper radiation, Cu$K\alpha$ = 0.154 178 nm. The recording of the small angle scattering films took from 24 h to a week. The sample-to-film distance was 351.0 mm. Once developed the films were measured on a Joyce Loebel microdensitometer. Each film was measured at least three times then the results were averaged.

2.6. Determination of the lamellar thickness

We applied the method used by Blundell and Osborn for the calculation of the lamellar thickness l_c for the various samples [25]. They were calculated from the value of the long period, L, obtained from small angle X-ray scattering traces and from the degree of crystallinity determined by X-ray diffraction, X_x, according to the following equation

$$l_c = L X_x \quad (4)$$

The use of X_c, X_h, or ϕ_c in Equation 4 leads to values of l_c slightly higher than those reported in the literature [25].

3. Results

3.1. Polymer characterization

The X-ray diffraction traces of selected film samples crystallized at various temperatures T_c from the glass and from the melt are reproduced in Fig. 1. The traces show a sharpening and an increase in the intensity of diffraction peaks indicating an increase in the degree of crystallinity as the crystallization temperature increases for the samples crystallized from the glass. For the series of samples crystallized from the melt, it was not possible to measure accurately significant differences in crystallinity between the samples based on the X-ray diffraction traces (see Table I).

One of the consistent features observed for both series is a change in the unit cell parameters with crystallization conditions. The crystallographic data reported in Table II show that the unit cell dimensions decrease with increasing T_c, with the value of the parameter a decreasing at a faster rate than b or c. Similar changes in unit cell parameters have been recently reported [28, 29]. Consequently, the volume of the unit cell decreases as a function of T_c for both series of samples crystallized from the glass and from the melt. Interestingly, Table II indicates that, for a given crystallization temperature, the samples crystallized from the melt have a slightly smaller volume than those crystallized from the glass. These variations in unit cell volume have a significant effect on the calculated density of a 100% crystalline material which increases by more than 3% from $T_c = 180\,^{\circ}C$ to $T_c = 340\,^{\circ}C$. This, in turn, significantly affects the calculation of the weight fraction and volume fraction crystallinity indices. The data obtained with respect to the characterization of the samples in terms of density, enthalpy of fusion, and degree of crystallinity are tabulated in Table I. It should be emphasized that the values for X_c have been corrected for the change in unit cell dimensions with T_c.

Not surprisingly, the crystallinity indices measured via density, enthalpy of fusion and X-ray diffraction are not the same. This is to be expected since each method measures slightly different characteristics of the material. A linear relationship can, however, be established between all of them when taken pairwise. The only data that can be considered as difficult to rationalize at this point are the slightly lower values of the experimental enthalpy of fusion Δh_{exp} for the samples crystallized from the melt ($\sim 43\,J\,g^{-1}$) compared to the corresponding samples crystallized from the glass ($\sim 50\,J\,g^{-1}$). One explanation for this behaviour could be related to the degree of perfection of the crystals and the contribution of the folds to the enthalpy of melting. Melting and recrystallization suspected to occur during the recording of the DSC as the sample is heated can also play a role here [33]. A thorough discussion of this observation is however beyond the scope of this paper.

3.2. Hardness measurements

For each individual sample at least 20 measurements were performed. No significant variation in microhardness over the surface of a given sample (which

would have indicated a high level of anisotropy) was observed. In addition, no preferential orientation was detected based on comparison of the lengths of the two diagonals of the indent which were always found to be equal within the experimental error.

Since polymers show a distinct creep effect during indentation, a series of microindentation measurements were performed on samples crystallized at 207 and 325 °C. The microhardness for these samples was measured for various indentation times over an interval of 5 s to 20 min. The results are plotted on Fig. 2. Due to the creep effect, an increase in the dimensions of the indent with longer indentation time is observed and consequently a lower microhardness value. This decrease can be mathematically expressed as

$$H = H' t^{-\beta} \quad (5)$$

where t is the indentation time, β a "creep" parameter and H' the hardness at $t = 0$ [16]. From a plot of $\log H$ against $\log t$ one obtains H' from the intercept and β from the slope. The intercept at $t = 0$ is of course different for the different samples but we found similar values for β (0.0346 and 0.0342) for the samples crystallized at 207 and 325 °C, respectively. These results indicate that, although there is a creep effect, this effect is about the same for all samples since β does not change significantly as a function of T_c. Consequently, all the microhardness values reported were measured with the same indentation time of 5 s.

The values of the microhardness for PEEK films crystallized under various conditions are also reported in Table I. They range between 135 MPa for the untreated Stabar film to approximately 290 MPa for the samples crystallized at the highest temperatures. These values indicate that PEEK is softer than poly(ethylene terephthalate) but harder than any other polymers which have been reported in the literature either in the review article by Eyerer and Lang [34] or by other authors who studied individual polymers. For comparison, in Table III are tabulated the hardness values of some of the polymers that appeared in the literature subsequent to the article by Eyerer and Lang [34]. Care should be taken, however, in comparing these numbers since the samples were not necessarily prepared by the same method and could have different degrees of crystallinity.

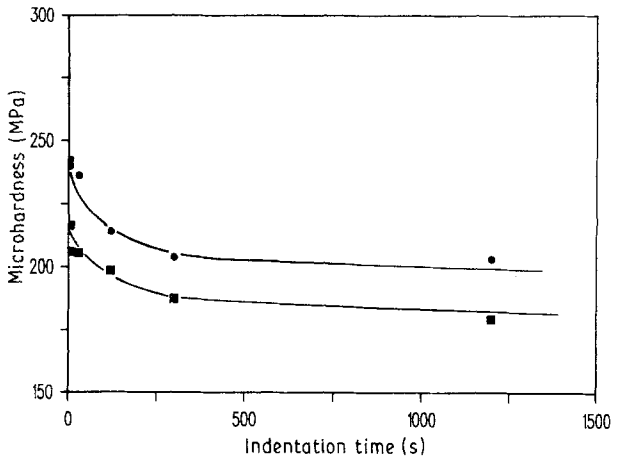

Figure 2 Microhardness values plotted against indentation time for samples crystallized from the glass at 207 °C (■) and 325 °C (●).

TABLE III Hardness values of various polymer measured by microindentation

	Hardness (MPa)	Reference
Polyethylene	88	[9]
Polyethylene (ultra oriented)	180	[6]
Polystyrene	230	[16]
Polypropylene	140	[18]
Poly(ethylene terephthalate)	500	[19]
Polytetrafluoroethylene	110	[19]
Polycarbonate	130	[20]
Polyparaphenylene	120	[23]
Poly(paraphenylene sulphide)	150	[23]
Poly(ether–ether–ketone)	290	this work

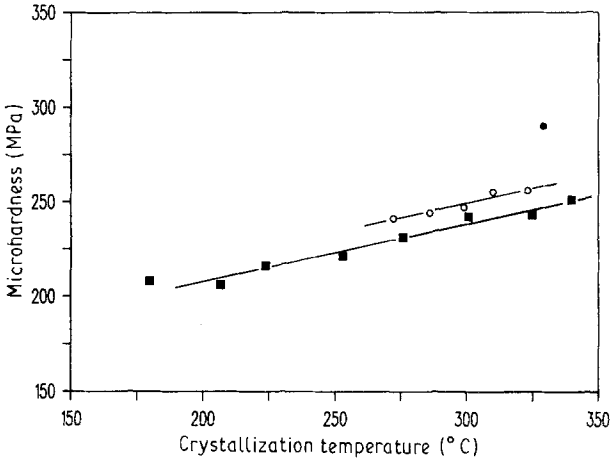

Figure 3 Evolution of microhardness as a function of crystallization temperature for the series crystallized from the glass (■), the melt (○) and the sample annealed for 17 h (●).

The effect of the crystallization temperature on microhardness is illustrated in Fig. 3 where H is plotted against the crystallization temperature T_c for each series crystallized for 1 h from the melt and from the glass. Two parallel straight lines can be drawn with the samples crystallized from the melt having higher values than those crystallized from the glass. This slightly higher hardness value is probably related to the improved crystal perfection as well as to the slightly higher degree of crystallinity of the former series. The sample crystallized from the melt, at 329 °C, for 17 h displays a higher hardness.

The plot of H against density for both polymer series, including the untreated amorphous Stabar film, gives a straight line, with a coefficient of correlation of 0.993 (see Fig. 4). All but one point, (the exception being the sample which was crystallized from the melt at 329 °C), fall on the same line. This particular sample displays a significantly higher microhardness probably because of the longer "annealing" time. This point is displayed for information only and is not included in the linear regression calculation. It suggests, however, an important effect of annealing time on the morphology and consequently on the microhardness of PEEK, a topic that is to be studied

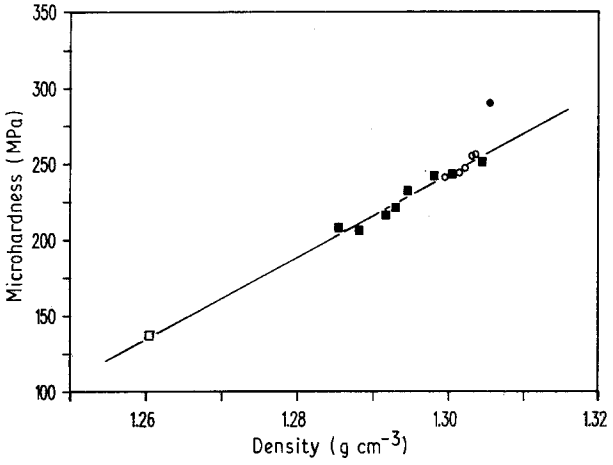

Figure 4 Linear relationship observed when microhardness is plotted against density. Only the sample annealed for 17 h does not fall on the line. (□ original (amorphous) film, ■ from the glass (1 h), ○ from the melt (1 h), ● from the melt (17 h))

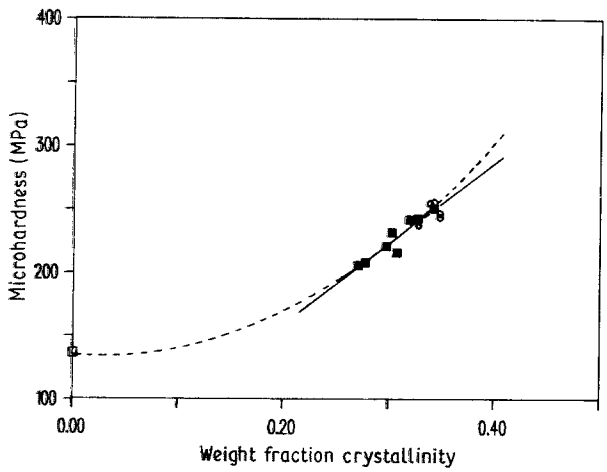

Figure 5 Plot of the microhardness against weight fraction crystallinity for the samples crystallized from the glass (■) and the melt (○), including the untreated amorphous film (□). The broken curve represents the best fit for all the data points taken altogether.

further. The behaviour of the curve in Fig. 4 is not surprising based on a comparison with other polymers. For example, microhardness is often correlated to the yield stress of the materials [1] and Popli and Mandelkern [28] have shown a linear relationship between yield stress and density and degree of crystallinity for polyethylene.

The dimensions of the unit cells of PEEK change with crystallization temperature, thus a linear relationship between hardness and degree of crystallinity is not expected. Fig. 5 shows that, when the data are plotted as hardness against weight fraction degree of crystallinity, a straight line (solid line) can be drawn if the data point for the amorphous sample is not considered. A second-order linear regression (broken line), with a coefficient of correlation of 0.981, seems, however, to describe better the data when the amorphous sample is included.

4. Discussion

4.1. Correlation with density and degree of crystallinity

The increase in microhardness with density and crystallinity is not surprising in light of the two deformation mechanisms of semicrystalline polymers occurring during indentation, as suggested by Balta–Calleja [1]. For samples with relatively low crystallinity, compression of the disordered molecular regions will be responsible for plastic deformation below the indentor. In this case, work has to be done against the steric hindrance to bond rotation of the molecules in the amorphous regions. At higher levels of crystallinity, the deformation modes of the crystals predominate and the strength of the crystals determine the overall mechanical properties of the polymer. Based on the density and X-ray diffraction data, an increase in the total crystallinity of the samples is observed as T_c increases, as well as a possible improvement in the crystalline perfection (the peaks in Fig. 1 are sharper for samples crystallized at higher T_c). It is believed that this healing of the crystalline defects occurring at higher temperature [9, 35], is related to a mechanism involving the diffusion of solid defects toward the surface layer of the crystallites [36], improving the packing of the chains. This explanation is also consistent with the decrease of the unit cell parameters as T_c increases (Fig. 2). Since the thickness of the lamellae also increases with increasing crystallization temperature [25], the overall increase in microhardness with T_c can be partly explained by the compounded effect of the presence of a greater number of thicker lamellar crystals having a larger equilibrium cohesive energy which oppose a greater resistance to plastic compression under the indentor.

Although it is possible, by extrapolation of the curve on Fig. 5, to estimate the microhardness of a completely crystalline sample, such a long range extrapolation should be very cautiously interpreted, since no experimental data point for $X_c > 0.5$ is available (it is not possible to crystallize PEEK to a degree of crystallinity higher than 0.5) [25]. One cannot, therefore, verify whether the hardness will continue to increase as the degree of crystallinity increases or if a plateau will be encountered. The extrapolation might, however, be justified based on the data obtained on polyethylene where a continuous increase in microhardness has been observed with increasing density [1]. A decrease in the slope of the curve was observed as density approached the density of a completely crystalline sample. For this reason we decided to undertake the extrapolation of the curve using both the linear fit (without the amorphous component) and the second-order fit. The linear curve yields a value of $H = 650$ MPa. This value is about 5 times higher than the microhardness of crystalline polyethylene. When compared with the microhardness of the completely amorphous PEEK film it is found to be only 5 times higher. This strongly contrasts with the case of polyethylene, where the extrapolated value for the ideal crystal was reported to be more than 150 times greater than the values for the ideally amorphous matrix [1]. This difference in the ratio of the microhardness of the pure crystalline component to the pure amorphous

component is probably associated with differences in the intrinsic flexibility of the respective polymer chains and their interactions with neighbouring chains. PEEK chains are likely to be much stiffer than polyethylene chains at room temperature since they are below T_g and are, therefore, likely to exert a stronger resistance to the diamond indentor, even when it is not incorporated into a crystal. Although PEEK is not characterized by a liquid crystalline behaviour [37], FTIR studies by Nguyen and Ishida [38] have confirmed the presence of local order in the amorphous phase of PEEK. We should also comment that the X-ray trace of the amorphous film shows a relatively intense amorphous halo which might also indicate a level of organization of the chain in the non-crystalline solid component. This ordering could contribute to the hardness of the amorphous component of the material. From the second-order fit, the hardness of a fully crystalline sample when extrapolated to $X_c = 1$ yields a value of 1100 MPa.

The extrapolated values of either 650 or 1100 MPa for the microhardness of the fully crystalline polymer are reasonable in the light of the calculated value of S_o, the ideal shear strength of a van der Waals solid, normal to the chain axis. During the indentation, the cohesive forces between the molecules have to be overcome to separate them and plastically deform the polymer crystal. The value of S_o can be calculated from the equation derived by Balta–Calleja [1] based on the Thomas–Stavely relation [39]

$$S_o = \frac{A^{1/2}(\Delta h_f)\gamma}{\delta l} \quad (6)$$

where A is the chain cross-section in the crystalline phase, Δh_f the heat of fusion, γ a constant equal to 0.12 and δl the displacement between adjacent molecules within the crystal sufficient for lattice destruction. Obviously the value of S_o depends on the choice of δl. Similarly to Balta–Calleja, we have used $\delta l = 0.1$ nm to calculate S_o [1]. Taking $\Delta h_f = 130\ J\ g^{-1}$ and calculating A from the unit cell parameters for the sample crystallized at 340 °C (see Table I) we obtained $S_o = 900$ MPa, which falls between the two extrapolated value of 650 and 1100 MPa.

4.2. Microhardness of the crystalline fraction

The unit cell parameters as well as the thickness of the lamellae change with temperature, thus it is appropriate to try to calculate the hardness of the crystalline component in each sample. This is possible by assuming a simple two phase model for semicrystalline polymers, where crystallized lamellae are separated by amorphous disordered region. Using such a model, Balta–Calleja has derived an empirical relationship for the microhardness H of a polymer

$$H = \alpha H_c + (1 - \alpha)H_a \quad (7)$$

where H_c and H_a are the microhardness values of the crystalline and the amorphous phase respectively and α a parameter related to the degree of crystallinity of the material [1]. Using the measured values for the degree of crystallinity and the value of 135 MPa for the hardness of the amorphous untreated Stabar film, it is, therefore, possible to calculate the value of H_c for each sample crystallized under different conditions. A problem arises here because various possibilities exist for the choice of the parameters describing α. Volume fraction [10], weight fraction [22], and molar fraction crystallinities [40] have all been used by various authors. We have performed the calculations using both volume fraction and the weight fraction crystallinity measured by density. The resulting H_c values are tabulated in Table IV. Although the two sets are numerically different, they both show a similar trend, i.e. the hardness of the crystalline component increases as the temperature of crystallization increases, therefore, as T_c increases, not only does the degree of crystallinity increase, but also the microhardness of the crystalline component. This is a consequence of the increase in thickness of the crystalline lamellae and the improvement in packing density of the chains in the unit cell. Consequently, we have attempted to continue our analysis of the data by trying to consider independently these two parameters.

4.3. Effect of lamellar thickness

The variation in microhardness of the crystalline phase H_c of a polymer can be predicted as a function of the average lamellar thickness l_c according to the following relationship derived from thermodynamic considerations by Balta–Calleja and Kilian [11, 40]

$$H_c = H_o/[1 + (b_1/l_c)] \quad (8)$$

where H_o is the microhardness of an infinitely thick crystal and b_1 a constant which is correlated to the volume–surface ratio of the mosaic crystal blocks prior to deformation. After rearranging, one obtains

$$\frac{1}{H_c} = \frac{1}{H_o} + \frac{b_1}{H_o}\frac{1}{l_c} \quad (9)$$

TABLE IV Microhardness of the crystalline component calculated using Equation 7 for the volume and weight fraction crystallinity determined by density

T_c (°C)	H_c (MPa)	
	volume fraction crystallinity	weight fraction crystallinity
From the glass		
180	413	398
207	414	398
224	415	400
253	443	424
276	477	456
301	494	470
325	489	466
340	498	474
From the melt		
272	482	460
286	469	449
299	480	458
310	516	490
323	514	489
329	643	605

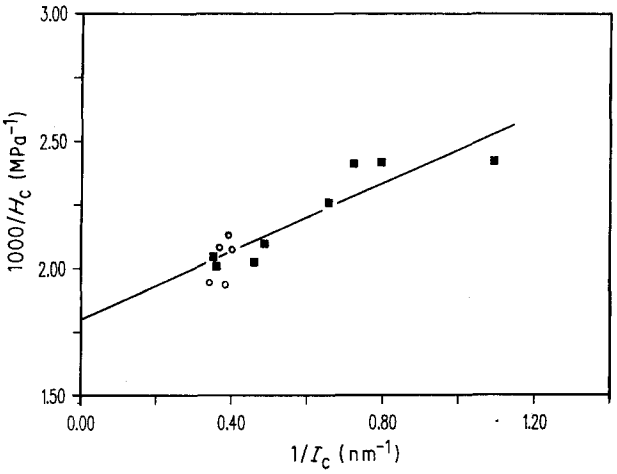

Figure 6 Plot of $1000/H_c$ against $1/l_c$ for the samples crystallized from the glass (■) and from the melt (○). The solid line is the best least square fit for both series of points taken altogether.

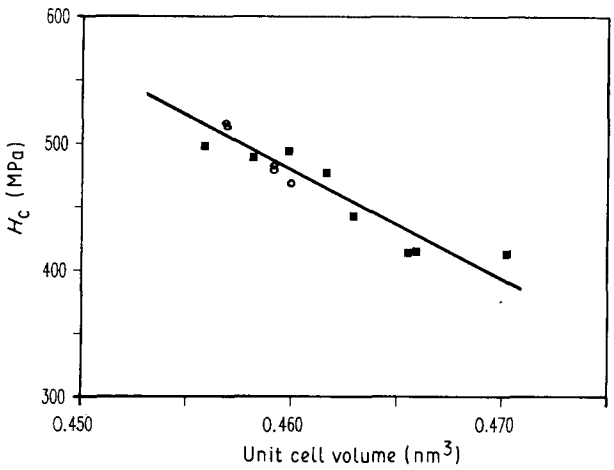

Figure 7 Evolution of the microhardness of the crystalline phase, H_c as a function of the volume of the unit cell of the crystals. Crystallized from the glass (■), from the melt (○).

A plot of $1/H_c$ against $1/l_c$ should, therefore, yield a straight line with the intercept corresponding to $1/H_0$ and the slope to b_1/H_0, from which both b_1 and H_0 can be calculated. Such a plot is shown on Fig. 6. All the data points fall relatively well on a unique straight line (solid line) which yields $H_0 = 550$ MPa and $b_1 = 3.9$ nm. This experimental value of H_0 is much lower than 900 MPa that can be eventually expected based on theoretical predictions as discussed earlier. This is an indication that the crystals have a poor internal molecular organization which is likely to improve with annealing. The value of $b_1 = 3.9$ nm is difficult to interpret in the light of only one series of samples. This parameter, which is supposed to be a constant for a polymer crystallized under specific conditions is correlated to the volume–surface ratio of the mosaic blocs making up the lamellae. Its value here is relatively small compared with the value obtained for polyethylene where $b_1 = 20$ nm when crystallized from the melt and 10 nm when crystallized under pressure [11].

4.4. Effect of chain packing

The variation of the unit cell dimensions of PEEK with temperature suggests that something other than the lamellar thickness or the mosaic block characteristics might be affecting the microhardness of the crystalline component. Better packing of the chains, and therefore changes in cohesive energy of the crystals could play a role. When the microhardness was plotted as a function of unit cell volume (Fig. 7), a linear relationship was obtained showing a decrease in hardness with increasing volume. Note that this plot was constructed without taking into consideration the different lamellar thickness of each sample. In that sense, both Figs 6 and 7 show the same trend. This similar behaviour is not surprising since both lamellar thickness and packing density are increasing with crystallization temperature.

It does not seem possible at the moment to separate the two contributions based on our current data. A series of samples having the same lamellar thickness but different unit cell dimensions would probably be useful here. The generation of such samples would be possible by crosslinking a series of samples previously crystallized and then annealing at different temperatures. The crosslinking which would take place in the interlamellar amorphous phase and would hinder subsequent lamellar thickening during further annealing but would not affect the change in volume of the crystalline phase. The resistance of PEEK to radiation as well as the unknown effect of the change in microhardness of the amorphous phase after crosslinking will certainly complicate such an experiment. We are presently conducting a preliminary investigation of the feasibility of such a study.

The limited amount of data available here is certainly insufficient to undertake any further meaningful quantification of the effect of morphology on microhardness. In order to relate microhardness and, for example, intermolecular forces, a knowledge of the intermolecular distances must be derived from X-ray diffraction data [10]. Although these distances were derived by Fratini *et al.* [41] for one particular unit cell having dimensions $a = 0.783$, $b = 0.594$ and $c = 0.986$ nm, they would have to be calculated for each sample in order to take into account the changes in unit cell parameters with crystallization temperature. Clearly, such a calculation would necessitate a thorough study which is obviously beyond the scope of this paper. In addition, the contribution of other subtle factors which are very difficult to evaluate such as the crystallite thickness distribution, the structure and relative amount of both the interfacial region and the residual non-crystalline region are known to affect the mechanical behaviour of polymers [29].

5. Conclusion

This relatively short series of experiments performed on samples prepared from one commercial PEEK film has demonstrated that microhardness can be correlated with some of the morphological features of PEEK. The study has shown the following.

1. A linear relationship between microhardness and density can be established for samples crystallized at various temperatures from the glass and the melt. When plotted against degree of crystallinity, the linear relationship does not apply since the unit cell dimensions of the crystals change with T_c. Extrapolation to a fully crystalline sample yields values which are in good agreement with the theoretical value of about 900 MPa calculated based on Equation 6.

2. The microhardness of the crystalline phase, H_c, of these semicrystalline samples can be calculated if the degree of crystallinity is known and assuming that the hardness of the amorphous Stabar film is an accurate measure of the microhardness of the amorphous phase.

3. A correlation between H_c and the lamellar thickness was established based on the Balta–Calleja and Kilian thermodynamic analysis [11, 40]. The analysis indicated that the mosaic blocs making up the lamellae have a slightly smaller volume–surface ratio than those of polyethylene. Also, microhardness increases as the unit cell parameters decrease, probably due to an increase in cohesive energy. Unfortunately the present data does not permit the resolution of the separate contributions of each factor.

4. It is suspected that long annealing times will eventually lead to an increase in microhardness through perfecting of the crystals.

Acknowledgements

The authors are grateful to Dr Moe Islam of the Mechanical Engineering Division for the use of the microindentor and to Dr Eric Gabe, Dr John Murray, Gerry Pleizier and Paul Toporowski of the Division of Chemistry for the help with the X-ray diffraction and density measurements and to Dr D. J. Carlsson and Dr M. Day for fruitful discussion during the study.

References

1. F. J. BALTA-CALLEJA, *Adv. Polym. Sci.* **66** (1985) 117.
2. J. BOWMAN and M. BEVIS, *Colloid Polym. Sci.* **255** (1977) 954.
3. F. J. BALTA-CALLEJA, *ibid.* **254** (1976) 258.
4. F. J. BALTA-CALLEJA and D. C. BASSETT, *J. Polym. Sci., Polym. Symposium* **58** (1977) 157.
5. F. J. BALTA-CALLEJA, W. T. MEAD and R. S. PORTER, *Polym. Eng. Sci.* **20** (1980) 393.
6. F. J. BALTA-CALLEJA, D. R. RUEDA, R. S. PORTER and W. T. MEAD, *J. Mater. Sci.* **15** (1980) 765.
7. F. J. BALTA-CALLEJA, J. MARTINEZ-SALAZAR, H. CACKOVIC and J. LOBODA-CACKOVIC, *ibid.* **16** (1981) 739.
8. J. MARTINEZ-SALAZAR and F. J. BALTA-CALLEJA, *ibid.* **18** (1983) 1077.
9. D. R. RUEDA, J. MARTINEZ-SALAZAR and F. J. BALTA-CALLEJA, *ibid.* **20** (1985) 834.
10. J. MARTINEZ-SALAZAR, J. GARCIA-PENA and F. J. BALTA-CALLEJA, *Polym. Commun.* **26** (1985) 57.
11. F. J. BALTA-CALLEJA and H. G. KILIAN, *Colloid Polym. Sci.* **263** (1985) 697.
12. F. J. BALTA-CALLEJA, D. R. RUEDA, J. GARCIA-PENA, F. P. WOLF and V. H. KARL, *J. Mater. Sci.* **21** (1986) 1139.
13. M. E. CAGIAO, D. R. RUEDA and F. J. BALTA-CALLEJA, *Colloid Polym. Sci.* **265** (1987) 37.
14. V. LORENZO, J. M. PERENA, J. M. G. FATOU, J. A. MENDEZ-MORALES and J. A. AZNAREZ, *J. Mater. Sci. Lett.* **6** (1987) 756.
15. V. LORENZO, J. M. PERENA, J. M. G. FATOU, J. A. MENDEZ-MORALES and J. A. AZNAREZ, *J. Mater. Sci.* **23** (1988) 3168.
16. B. L. EVANS, *ibid.* **24** (1989) 173.
17. J. MARTINEZ-SALAZAR and F. J. BALTA-CALLEJA, *J. Mater. Sci. Lett.* **4** (1985) 324.
18. F. J. BALTA-CALLEJA, J. MARTINEZ-SALAZAR and T. ASANO, *ibid.* **7** (1988) 165.
19. P. PARASHAR, B. BAJPAI, J. M. KELLER and S. H. DATT, *Makromol. Chem., Macromol. Symp.* **20/21** (1988) 465.
20. R. BAJPAI, J. M. KELLER and S. F. DATT, *ibid.* **20/21** (1988) 461.
21. J. MARTINEZ-SALAZAR, J. C. CANALDA-CAMARA, E. LOPEZ CABARCOS and F. J. BALTA-CALLEJA, *Colloid Polym. Sci.* **266** (1988) 41.
22. J. MARTINEZ-SALAZAR, J. M. GARCIA TIJERO and F. J. BALTA-CALLEJA, *J. Mater. Sci.* **23** (1988) 862.
23. D. R. RUEDA, F. J. BALTA-CALLEJA, J. M. AYRES DE COMPOS and M. E. CAGIO, *ibid.* **23** (1988) 4487.
24. J. BOWMAN, N. HARRIS and M. BEVIS, *J. Mater. Sci.* **10** (1975) 63.
25. D. J. BLUNDEL and B. N. OSBORN, *Polymer* **24** (1983) 953.
26. Y. LEE and R. S. PORTER, *Macromolecules* **20** (1987) 1336.
27. C. N. VELISARIS and J. C. SEFERIS, *Polym. Eng. Sci.* **26** (1986) 1574.
28. R. POPPLI and L. MANDELKERN, *J. Polym. Sci.: B: Polym. Phys.* **25** (1987) 441.
29. L. MANDELKERN, *Polym. J.* **17** (1985) 337.
30. Y. DESLANDES and E. ALVA ROSA, *Polym. Commun.* **31** (1990) 269.
31. N. T. WAKELYN, *J. Polym. Sci.: C: Polym. Lett.* **25** (1987) 25.
32. J. N. HAY, J. I. LANGFORD and J. R. LLOYD, *Polymer* **30** (1989) 489.
33. D. J. BLUNDELL, *ibid.* **28** (1987) 2248.
34. P. EYERER and G. LANG, *Kunstsoffe* **62** (1972) 322.
35. E. W. FISHER and G. F. SCHMIDT, *Agnew. Chem.* **74** (1962) 551.
36. D. H. RENEKER and MAZUR, *J. Bull. Amer. Phys. Soc.* **26** (1981) 262.
37. H. X. NGUYEN and H. ISHIDA, *Polym. Compos.* **8** (1987) 57.
38. *Idem, Polymer* **27** (1986) 1400.
39. D. G. THOMAS and L. A. K. STAVELY, *J. Chem. Soc.* **1952** (1952) 4569.
40. F. J. BALTA-CALLEJA and H. G. KILIAN, *Colloid Polym. Sci.* **266** (1988) 29.
41. A. V. FRATINI, E. M. CROSS, R. B. WHITAKER and W. W. ADAMS, *Polymer* **27** (1986) 861.

Received 9 May
and accepted 26 June 1990